Expanded Methods

Materials and Reagents

Antibody: anti-SUV39H1 (D11B6, CST), anti-H3K9me3 (ab8898, abcam), anti-H3K9ac (ab32129, Abcam), anti-H3K4me3 (ab8580, Abcam), anti-H3K4ac (ab176799, Abcam), anti-H3K27me3 (ab6002, Abcam), anti-CBX3 (ab217999, Abcam), anti-RING1 (ab180170, Abcam), anti-KDM2A (ab191387, Abcam), anti-HDAC1 (ab280198, Abcam), anti-VERSICAN (ab19345, Abcam), anti-ADAMTS4 (ab185722, Abcam), anti-CSE (ab151769, Abcam), IgG (ab172730, Abcam), anti-α-SMA (ab7817, Abcam), anti-GAPDH (Af2823, Beyotime), anti-HA-HRP (H1103, LABLEAD), anti-His-HRP (H1104, LABLEAD), anti-Myc-HRP (M1102, LABLEAD), Anti-DDDDK tag (ab205606，Abcam).

pcDNA3.1-CSE, pcDNA3.1-CBX3-flag, pcDNA3.1-RING1-6his, pcDNA3.1-KDM2A-HA, pcDNA3.1-SUV39H1-strep, pcDNA3.1-HDAC1-myc, AAV9-sm22α-CBX3, AAV9-sm22α-CSE, AAV9-sm22α-GFP and rAAV8-HCRApoE/hAAT-D377Y-mPCSK9 (AV208001-AV8) were from WZ Biosciences lnc. Plasmid pcmv-CBX3 and pcmv-RING1B was from OriGene. AngII (A9525-50MG, SIGMA)), mini-pump (model 2004, Alzet), β-Aminopropionitrile (A3134, SIGMA). Paigen diet (D12109C, Research diets). siCBX3 (CCUGAAGAAUUUGUGGUAGAA) was from Shanghai primerna NAT co., Ltd.

Extravascular Stent Implantation Using a Collagen Sponge

The procedure began with a blunt dissection of the abdominal aorta between the diaphragm and the right renal artery, the intended site for AngII-induced murine abdominal aortic aneurysm (AAA) formation. Following dissection, an absorbable collagen sponge was implanted around the aorta to serve as an extravascular stent. To facilitate localized gene overexpression, 50 μL of sterile saline containing adeno-associated virus (AAV; 5×10^{11} genome copies) was applied directly to the collagen sponge. The abdominal incision was then closed and disinfected. Postoperatively, subcutaneous penicillin injections were administered for three days to prevent infection. After a one-week recovery period, the AngII infusion protocol for AAA induction was initiated.

Primary Culture of Vascular Smooth Muscle Cells

Primary vascular smooth muscle cells were isolated from 6–8-week-old male wild-type and cystathionine γ-lyase knockout (CSE-KO) mice. The cells were cultured in Dulbecco's Modified Eagle Medium (DMEM) supplemented with 20% fetal bovine serum (FBS; Gibco, #10099141C) and 10% penicillin-streptomycin (Pen Strep; Gibco, #15140-122). The culture medium was refreshed every two days, and cells were maintained in a humidified incubator at 37 °C with 5% CO_2 and 95% air. Primary VSMCs between passages three and eight were used for subsequent experiments.

Protein Extraction and Western Blot Analysis

Cells were lysed in RIPA buffer (Solarbio, #R0010) containing protease and phosphatase inhibitor cocktails. The lysates were centrifuged at 12,000 rpm for 10 minutes at 4 °C, and the supernatant was collected for protein quantification using a bicinchoninic acid (BCA) assay. Protein samples (20 μg per lane) were resolved by sodium dodecyl sulfate–polyacrylamide gel electrophoresis (SDS-PAGE) and subsequently transferred onto nitrocellulose membranes. The membranes were blocked with 5% non-fat milk for 1 hour at room temperature, followed by overnight incubation at 4 °C with primary antibodies targeting the proteins of interest. After washing with Tris-buffered saline containing Tween-20 (TBST), the membranes were incubated with horseradish peroxidase (HRP)-conjugated secondary antibodies for 1 hour at room temperature. Protein bands were visualized using a chemiluminescence detection kit following additional TBST washes.

RNA preparation and RT-qPCR analysis

Total RNA was extracted from treated samples using TRIzol® reagent (Invitrogen) according to the manufacturer's protocol, followed by DNase I treatment to eliminate genomic DNA contamination. RNA concentration and purity were verified spectrophotometrically (A260/A280 ratio $\geqslant$ 1.8). First-strand complementary DNA (cDNA) was synthesized from 1 μg of total RNA using a High-Capacity cDNA Reverse Transcription Kit (Thermo Scientific, #K1622) with random hexamer primers.Quantitative real-time PCR (qRT-PCR) was performed using SYBR Green PCR Master Mix kit (Yeasen Biotechnology, China). No-template controls (NTCs) and no-reverse transcription controls (NRTs) were included to rule out contamination and genomic DNA amplification, respectively. Relative gene expression was calculated using

the comparative 2-ΔΔCt method, with GAPDH serving as the endogenous reference. Primer sequences are provided in Supplementary Table 2.

siRNA and Plasmid Transfection

Vascular smooth muscle cells (VSMCs) were seeded in 6-well plates and transfected at approximately 70% confluency. Transfection was performed using 2 μg of plasmid or 200 nM siRNA mixed with Lipofectamine 3000 reagent (Thermo Fisher Scientific, #L3000075) according to the manufacturer's protocol. Following a 6-hour incubation period, the transfection medium was replaced with standard culture medium, and cells were cultured for an additional 48 hours before mRNA and protein expression levels were assessed.

Immunofluorescence Staining

Aortic Tissue Staining

Abdominal aortic aneurysm (AAA) specimens were fixed in 4% paraformaldehyde (PFA) immediately after isolation. After 24 hours of fixation, tissues were paraffin-embedded and sectioned. The sections were treated with 3% hydrogen peroxide to quench endogenous peroxidase activity. Antigen retrieval was performed by heating the sections in citrate buffer (95 °C, 20 min), followed by cooling to room temperature.

VSMC Staining

For cellular immunofluorescence, VSMCs were fixed in 4% PFA for 15 min at room temperature, washed three times with phosphate-buffered saline (PBS), and permeabilized with 0.5% Triton X-100 (15 min, room temperature).

Immunostaining Procedure

Both tissue sections and cells were blocked with 1% bovine serum albumin (BSA) for 1 hour, then incubated overnight at 4 °C with primary antibodies. After washing, samples were incubated with fluorophore-conjugated secondary antibodies for 1 hour at room temperature. Nuclei were counterstained with 4′,6-diamidino-2-phenylindole (DAPI) for 10 min. Fluorescence images were acquired using either a fluorescence microscope or confocal laser scanning microscope.

Histological and Immunohistochemical Analyses

Elastic Fiber Staining

Paraffin-embedded aortic sections were stained using an Aldehyde-Fuchsin Stain Solution Kit (Solarbio, #G1594) following the manufacturer's protocol. Elastic fiber morphology was subsequently examined by light microscopy.

Masson's Trichrome Staining

Aortic tissue sections were deparaffinized through xylene immersion and graded ethanol rehydration. Collagen deposition was assessed using a Masson's Trichrome Stain Kit (Sigma-Aldrich, #HT15-1KT) according to standard protocols, with final examination by light microscopy.

Hematoxylin & Eosin Staining and Immunohistochemistry

Tissue architecture was evaluated through conventional hematoxylin and eosin (H&E) staining. For immunohistochemical analysis, sections were first treated with 3% hydrogen peroxide for 10 minutes to quench endogenous peroxidase activity. Non-specific binding was blocked with 1% BSA for 1 hour at room temperature. Primary antibody incubation was performed overnight at 4°C, followed by detection using a Rabbit Polymer Detection System according to the manufacturer's instructions. After PBS washes, sections were developed with 3,3'-diaminobenzidine (DAB) for 2 minutes and counterstained with hematoxylin prior to microscopic evaluation.

TUNEL Apoptosis Assay

Apoptotic cells were identified in paraffin-embedded sections using a One-Step TUNEL In Situ Apoptosis Kit (Elabscience, #E-CK-A321) following the manufacturer's protocol. Fluorescent visualization was performed using an epifluorescence microscope equipped with appropriate filters.

RNA Sequencing Analysis

Total RNA was extracted using TRIzol reagent, followed by DNase I treatment and quality assessment (RNA Integrity Number≥8.0). Ribosomal RNA was depleted using the NEBNext rRNA Depletion Kit, and strand-specific cDNA libraries were prepared with the NEBNext Ultra™ II RNA Library Prep Kit. Libraries were quantified by Qubit and pooled for 150-bp paired-end sequencing on an Illumina NovaSeq 6000 platform.

Raw reads were quality-trimmed (Trimmomatic) and aligned to the reference genome (STAR aligner). Gene expression quantification was performed using featureCounts, followed by differential expression analysis (DESeq2; FDR < 0.05). Functional enrichment was assessed via GO and KEGG pathway analyses (clusterProfiler). Data had uploaded the Gene Expression Omnibus (GEO) database (GSE290627)

Chromatin Immunoprecipitation Sequencing (ChIP-seq)

Wild-type (WT) and knockout (KO) cells undergoing differentiation were stimulated with 1 μM AngII prior to crosslinking. Chromatin was fixed with 1% formaldehyde (v/v) for 10 min at room temperature, followed by quenching with 2.5 M glycine for 5 min. Cells were washed twice with ice-cold PBS, harvested by centrifugation (12,000 × g, 10 min, 4 °C), and lysed in RIPA buffer supplemented with protease and phosphatase inhibitors. Chromatin was sheared to 200–500 bp fragments using a Diagenode Bioruptor sonicator (30 sec ON/30 sec OFF cycles, 15 min total).

For immunoprecipitation, lysates were incubated overnight at 4 °C with antibodies targeting H3K9me3, H3K9ac, or H3K4me3 (1–5 μg per reaction), followed by capture with protein A/G magnetic beads. Beads were sequentially washed with: Low-salt buffer (20 mM Tris-HCl pH 8.1, 150 mM NaCl, 2 mM EDTA, 1% Triton X-100, 0.1% SDS), High-salt buffer (500 mM NaCl), LiCl wash buffer (10 mM Tris-HCl pH 8.1, 250 mM LiCl, 1 mM EDTA, 1% deoxycholate, 1% NP-40), TE buffer (10 mM Tris-HCl, 1 mM EDTA, pH 8.0). Immunoprecipitated DNA was eluted (1% SDS, 100 mM NaHCO3, 37°C, 30 min), reverse-crosslinked (200 mM NaCl, RNase A [TransGen, #GE101], 37°C, 30 min), and digested with Proteinase K (TransGen, #GE201; 65°C, 6 h). DNA was purified by phenol-chloroform extraction and ethanol precipitation.

Library preparation and sequencing were performed by LC-Bio Technologies (Hangzhou) using the Illumina NovaSeq 6000 platform (150 bp paired-end reads, ~30 million reads/sample). Raw data were processed through standard ChIP-seq pipelines for peak calling (MACS2) and differential binding analysis. Data had uploaded the Gene Expression Omnibus (GEO) database (GSE296864).

Co-immunoprecipitation Assay

HEK293T cells were co-transfected with pcDNA3.1-CBX3-Flag along with one of the following expression plasmids: pcDNA3.1-RING1-His, pcDNA3.1-SUV39H1-Strep, pcDNA3.1-HDAC1-Myc, or pcDNA3.1-KDM2A-HA, using Lipofectamine 3000 according to the manufacturer's protocol. After 24 hours, cells were lysed in RIPA buffer (Solarbio, #R0010) containing 1× protease inhibitor cocktail. Lysates were cleared by centrifugation (12,000 × g, 10 min, 4°C), and protein concentrations were determined using a BCA Protein Assay Kit (Thermo Fisher Scientific, #23225).

For immunoprecipitation, Dynabeads Protein G (Invitrogen, #10004D) were pre-incubated overnight at 4°C with 2 μg of the following antibodies: anti-CBX3, anti-KDM2A, anti-HDAC1, anti-SUV39H1, anti-RING1, or species-matched IgG control. Cleared lysates (500 μg total protein) were then incubated with the antibody-conjugated beads overnight at 4°C with gentle rotation.

Following incubation, beads were washed three times with ice-cold RIPA buffer. Bound proteins were eluted by boiling in 2× Laemmli buffer (95°C, 5 min) and analyzed by western blotting as previously described. Input lysates (10% of total) were included as positive controls for all experiments.

Supplementary Figure 1

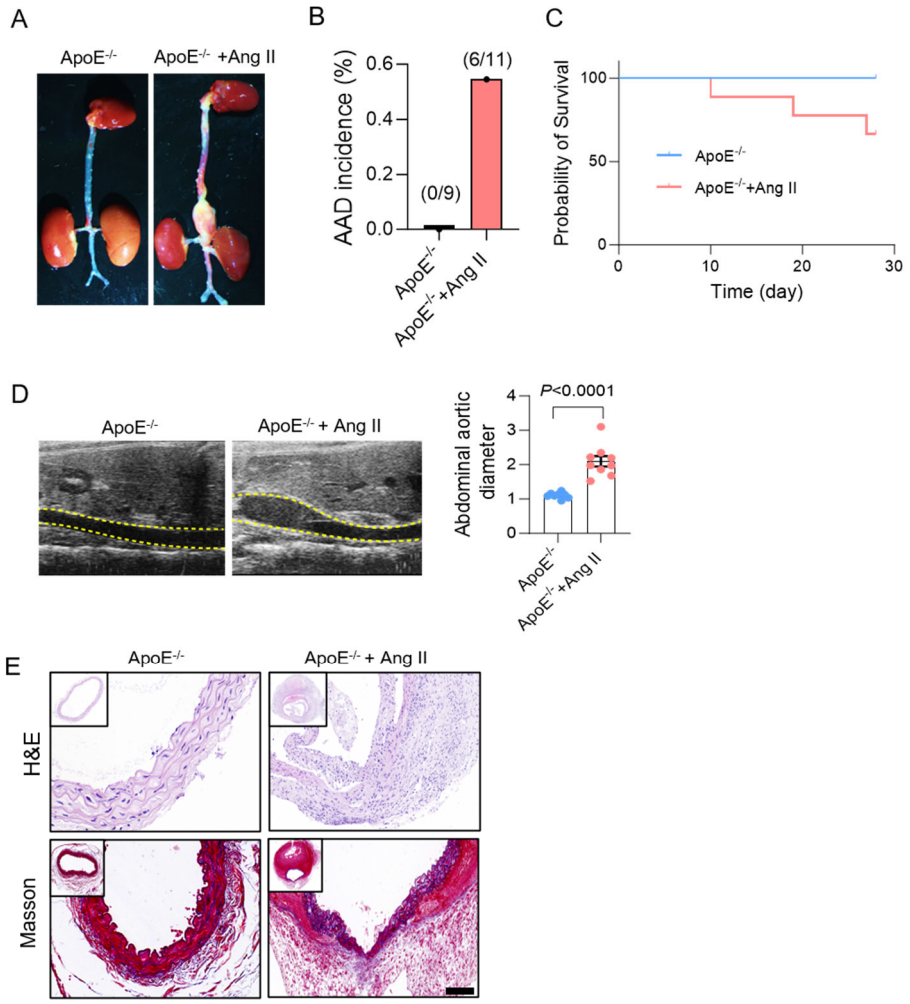

Supplementary Figure 1. Characterization of AngII-induced aortic aneurysm/dissection (AAD) in ApoE$^{-/-}$ mice.

(A) Representative macroscopic image of an AAD lesion induced by angiotensin II (AngII) infusion in ApoE-/- mice. (B) Incidence rate of AAA formation. (C) Kaplan-Meier survival curve of mice following AngII infusion. (D) Quantification of abdominal aortic diameter by echocardiography. (E) Histological analysis of aortic tissue by hematoxylin & eosin (H&E) and Masson's trichrome staining, demonstrating aneurysm formation and collagen deposition, respectively. Data are presented as mean ± SEM. Aortic diameter was analyzed using an unpaired two-tailed Student's t-test.

Supplementary Figure 2

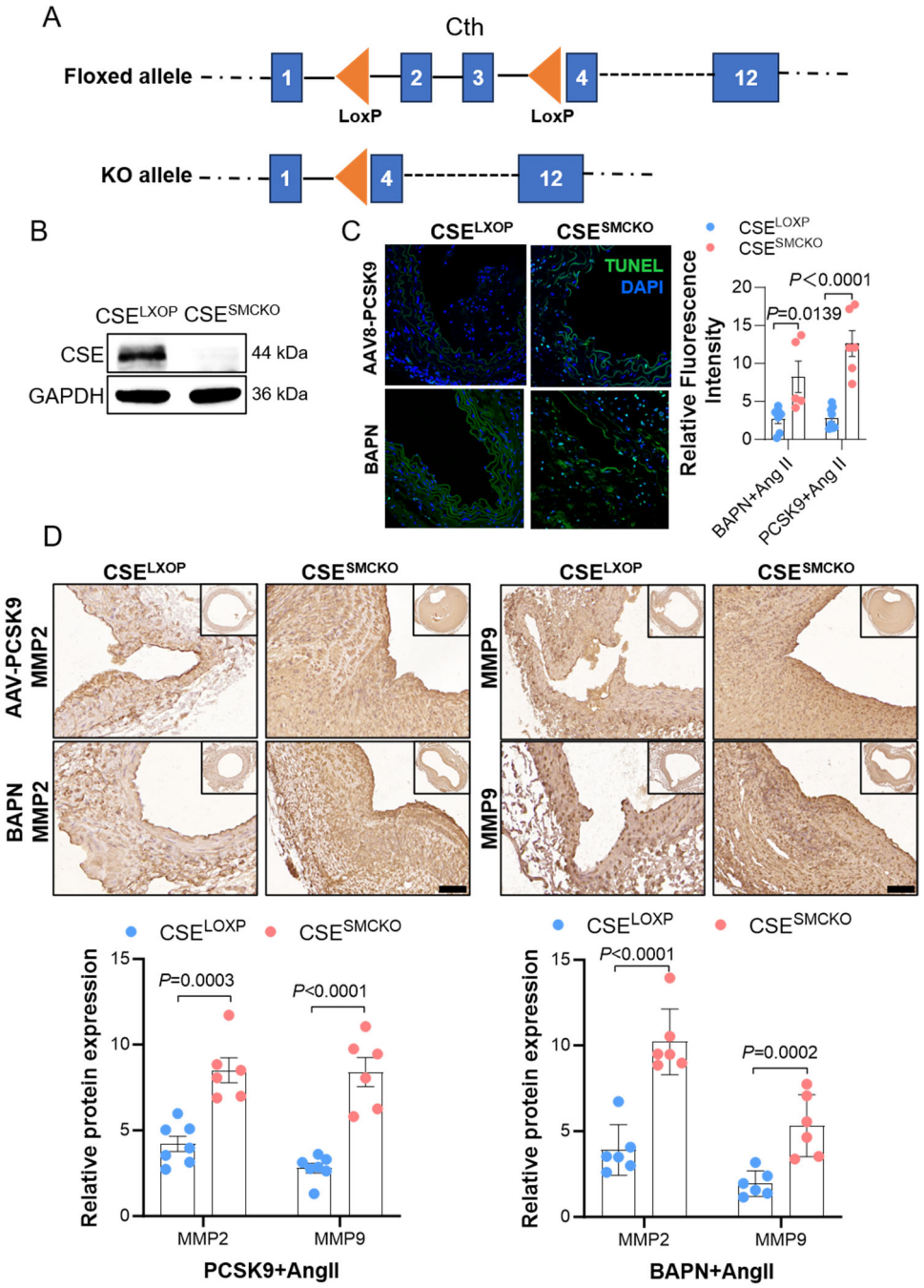

Supplementary Figure 2. VSMC-specific CSE deletion exacerbates apoptosis and MMP2/9 expression in AngII-induced AAA models.

(A) Schematic of the Cth gene targeting strategy, with LoxP sites flanking exons 2–3 to generate VSMC-specific Cth knockout (CSE^{SMCKO}) mice. (B) Western blot confirming CSE ablation in CSE^{SMCKO} VSMCs. (C) TUNEL staining demonstrating enhanced aortic smooth muscle cell apoptosis in CSE^{SMCKO} mice following AngII infusion. (D) Immunohistochemical analysis showing elevated MMP2 and MMP9 protein expression in aortic tissues of CSESMCKO mice subjected to AngII-induced AAA. Data are presented as mean ± SEM. The differences were analyzed using an unpaired two-tailed Student's t-test.

Supplementary Figure 3

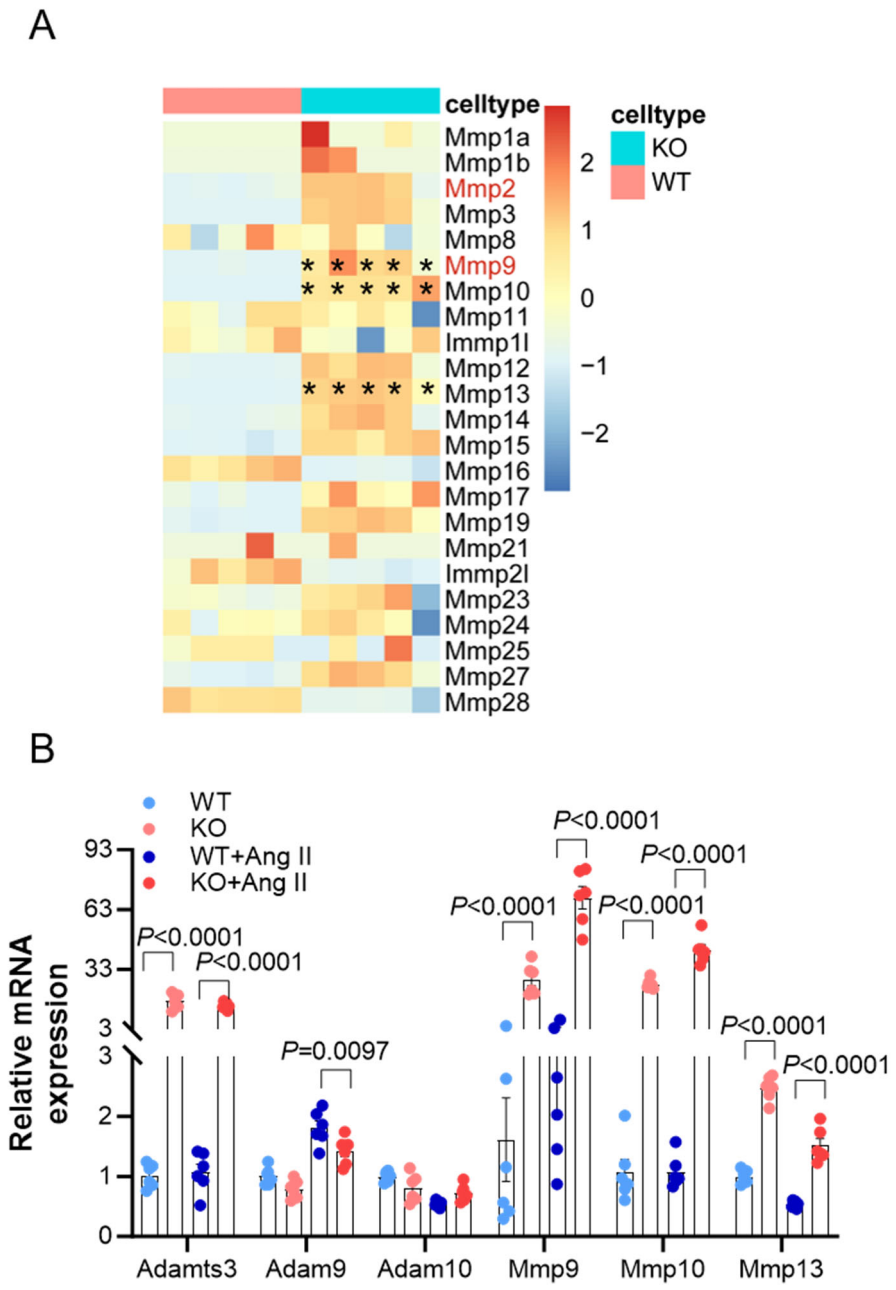

Supplementary Figure 3. Transcriptional alterations of MMP and ADAM family genes in CSE-deficient VSMCs.
(A) Heatmap depicting differentially expressed MMP family genes in CSE-deficient VSMCs based on RNA sequencing analysis (*P<0.05). (B) qRT-PCR validation of significant MMP and ADAM family gene expression changes identified in the RNA-seq dataset. Data were analyzed using two-way mixed-effects ANOVA followed by Tukey's multiple comparisons test.

Supplementary Figure 4

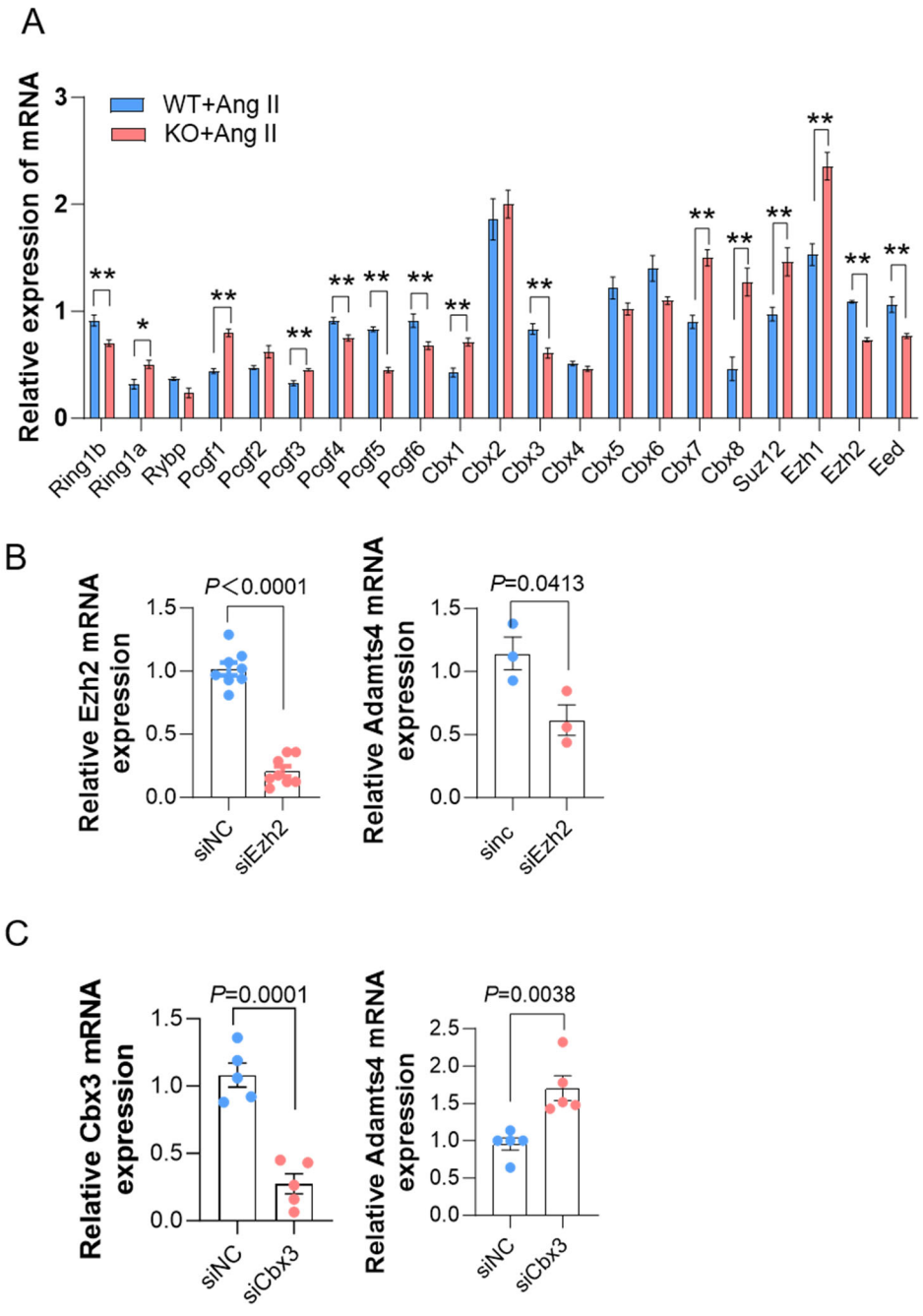

Supplementary Figure 4. Validation of gene expression alterations in CSE-deficient VSMCs by qRT-PCR.
(A) qRT-PCR analysis confirmed RNA sequencing results showing significant changes in PRC-related genes (*P<0.05, **P<0.01), including downregulation of Cbx3 and Ezh2 in CSE-deficient VSMCs. (B) Ezh2 knockdown decreased Adamts4 expression. (C) Cbx3 knockdown increased Adamts4 expression. Data represent mean ± SEM; statistical significance was determined by unpaired two-tailed Student's t-test.

Supplementary Figure 5

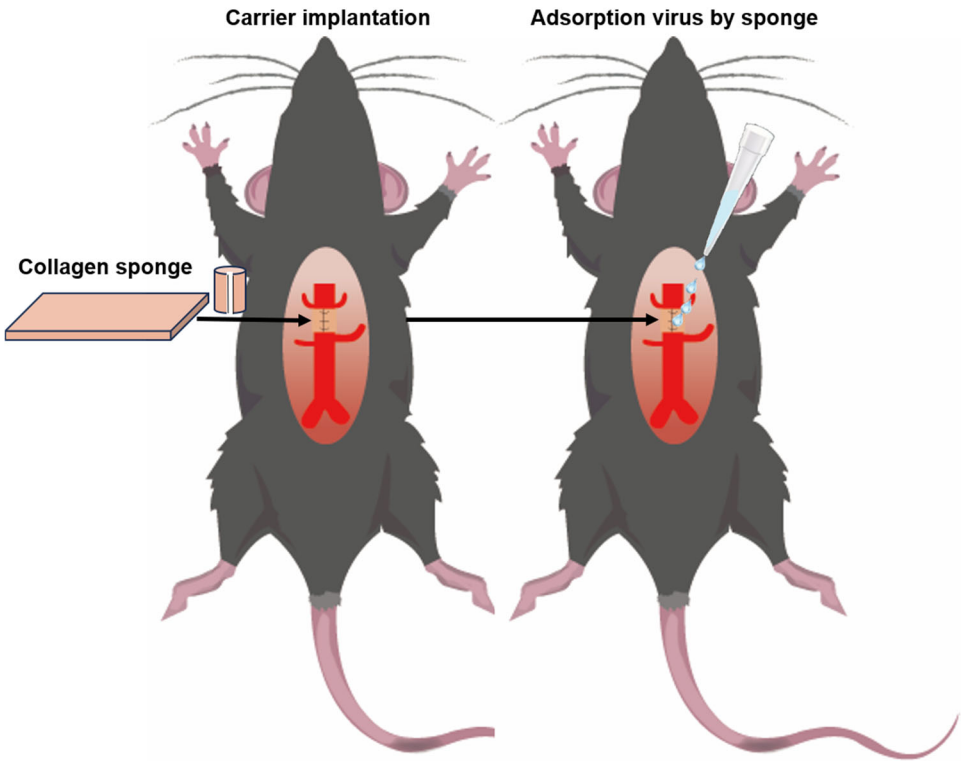

Supplementary Figure 5. Schematic representation of collagen-based extravascular stent implantation. Anatomical placement of the carrier between the diaphragmatic and renal arterial regions, circumferential aortic support. Localized viral delivery method showed AAV9 (5×10^{11} vg in 50 μl PBS) via sponge absorption for targeted CSE/CBX3 overexpression.

Supplementary Figure 6

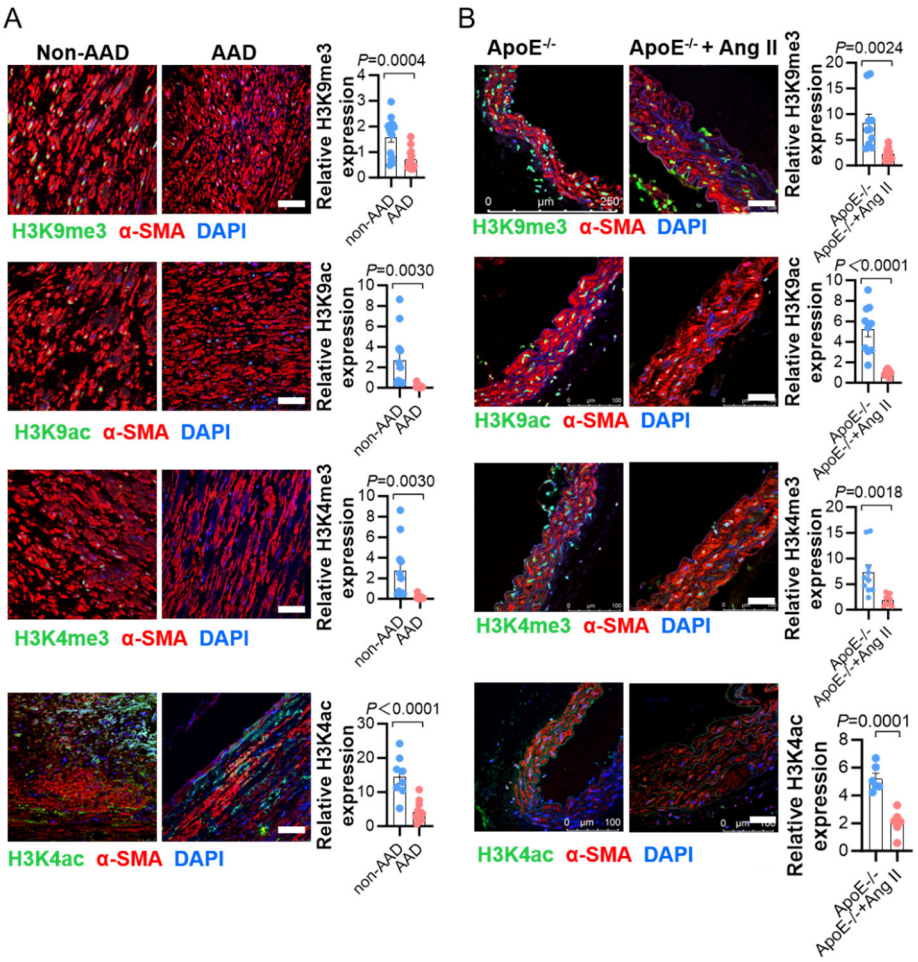

Supplementary Figure 6. Reduced H3K9me3/ac and H3K4me3/ac expression in human AAA tissues and AngII-induced AAA mice.

(A) Immunofluorescence staining revealed a significant decrease in H3K9me3, H3K9ac, H3K4me3, and H3K4ac levels in the aneurysm regions compared to non-aneurysmal areas of human AAA patient samples. (B) Similarly, aortic VSMCs from AngII-induced ApoE-/- AAA mice exhibited reduced expression of H3K9me3, H3K9ac, H3K4me3, and H3K4ac. Data are presented as mean ± SEM; statistical significance was assessed using an unpaired two-tailed Student's t-test.

Supplementary Figure 7

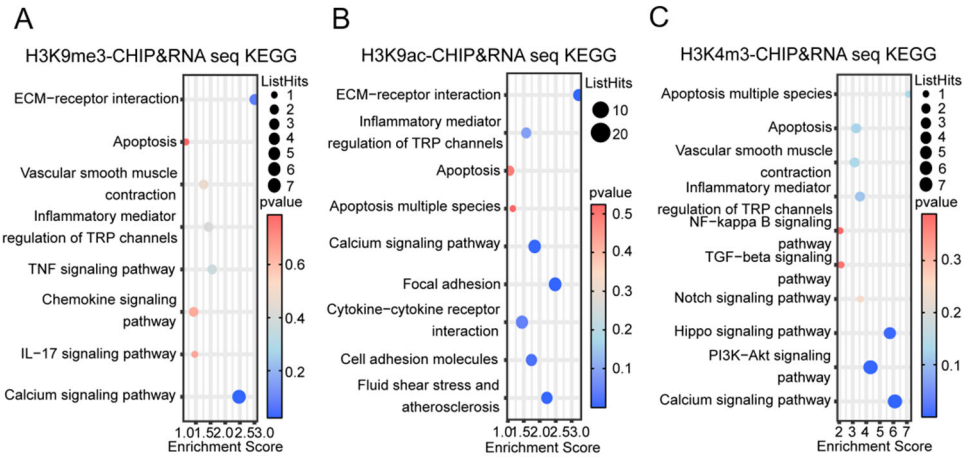

Supplementary Figure 7. KEGG pathway enrichment analysis of genes overlapping between ChIP-seq targets and RNA-seq differentially expressed genes.

KEGG pathway analysis was performed on genes that overlapped between (A) H3K9me3 ChIP-seq targets, (B) H3K9ac ChIP-seq targets, and (C) H3K4me3 ChIP-seq targets and differentially expressed genes from RNA-seq. Enriched pathways are shown for each histone modification-associated gene set.

Supplementary Figure 8

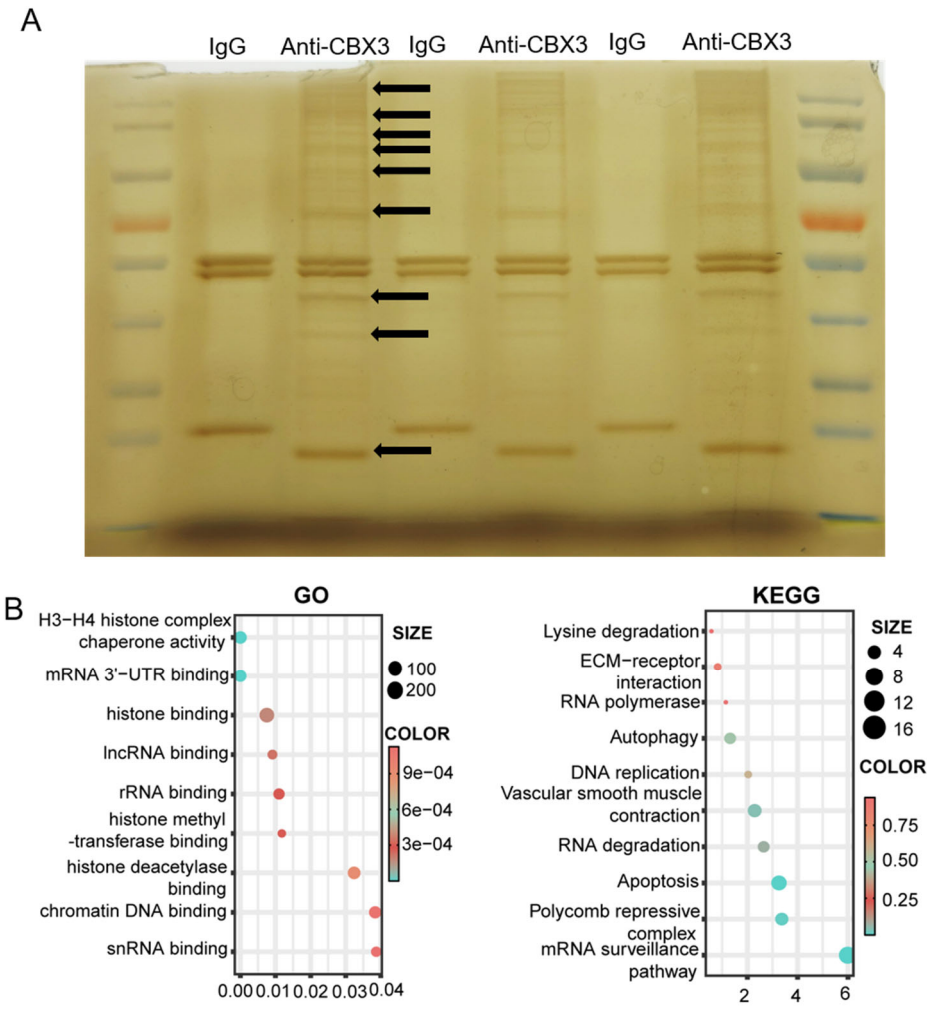

Supplementary Figure 8. Proteomic identification of CBX3-interacting proteins and their functional enrichment analysis.

(A) CBX3-associated protein complexes were immunoprecipitated using a CBX3-specific antibody, separated by SDS-PAGE, and visualized by silver staining. Differential protein bands (indicated by black arrows) were excised for mass spectrometry-based proteomic analysis. (B) GO and KEGG pathway enrichment analyses of the identified CBX3-interacting proteins.

Supplementary Figure 9

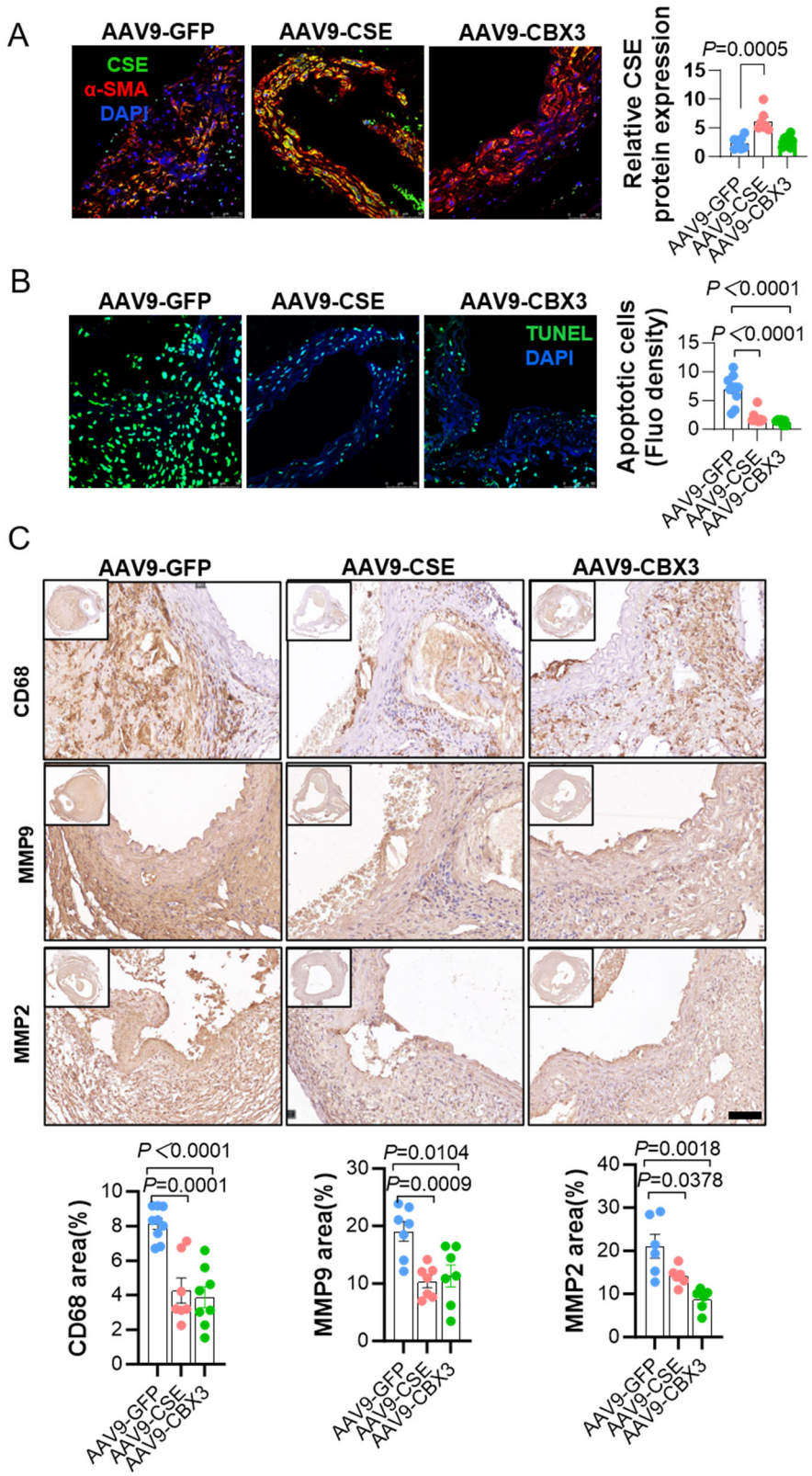

Supplementary Figure 9. Local aortic overexpression of CSE or CBX3 attenuates apoptosis, macrophage infiltration, and MMP2/9 expression in AAA.
(A) Immunofluorescence staining confirmed successful CSE and CBX3 (Figure 9D) overexpression in the aortic wall of AngII-induced ApoE$^{-/-}$ AAD mice following local

gene delivery. (B) TUNEL staining demonstrated that both CSE and CBX3 overexpression significantly reduced vascular cell apoptosis compared to controls. (C) Immunohistochemical analysis revealed decreased macrophage infiltration and reduced expression of MMP2 and MMP9 in the aneurysmal regions of CSE- or CBX3-overexpressing mice. Data represent mean ± SEM; statistical significance was determined by one-way ANOVA with post-hoc testing.

Supplementary Figure 10

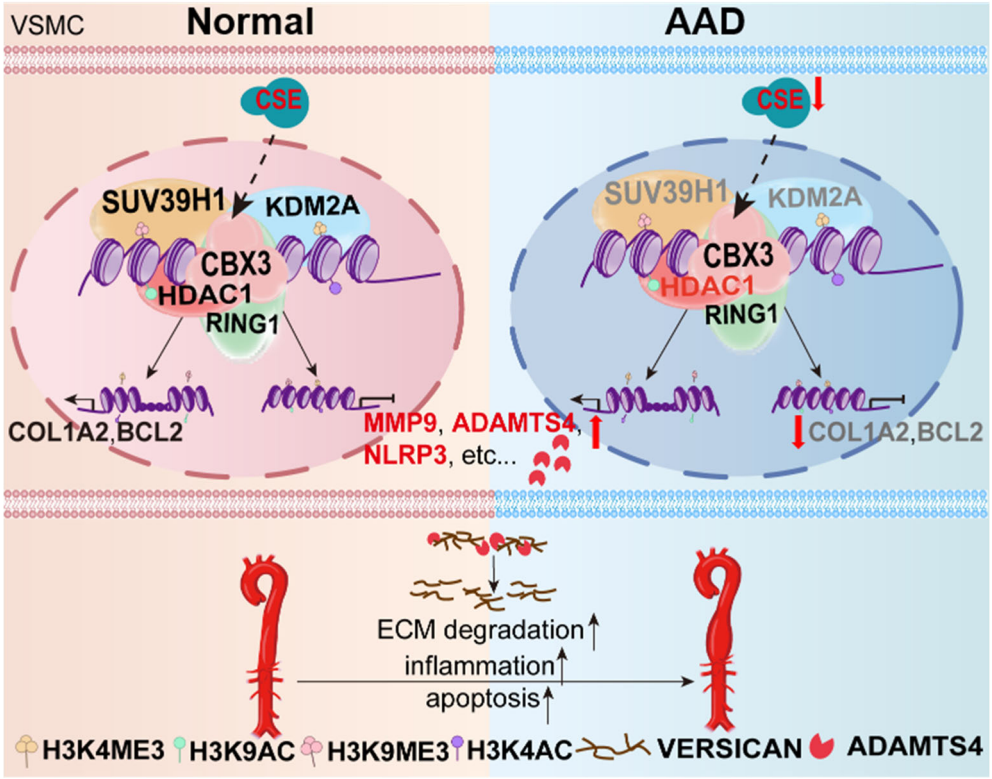

Figure 10. Schematic summary of the proposed mechanism underlying CSE in AAD pathogenesis. Downregulation of CSE expression in VSMCs reduces CBX3 expression, leading to diminished binding of CBX3 to SUV39H1 and KDM2A, along with increased HDAC1 binding. These changes result in decreased H3K9me3/ac and H3K4me3/ac levels, disrupting the transcription of target genes primarily enriched in ECM remodeling, apoptosis, and inflammation. For instance, elevated ADAMTS4 expression promotes versican degradation, thereby contributing to AAA development and progression.